Plasma Perspective on Strong-Field Multiphoton Ionization

P. B. Corkum
National Research Council of Canada, Ottawa, Ontario, Canada K1A 0R6
(Received 9 February 1993)

During strong-field multiphoton ionization, a wave packet is formed each time the laser field passes its maximum value. Within the first laser period after ionization there is a significant probability that the electron will return to the vicinity of the ion with very high kinetic energy. High-harmonic generation, multiphoton two-electron ejection, and very high energy above-threshold-ionization electrons are all consequences of this electron-ion interaction. One important parameter which determines the strength of these effects is the rate at which the wave packet spreads in the direction perpendicular to the laser electric field; another is the laser polarization. These will be crucial parameters in future experiments.

PACS numbers: 32.80.Rm

This paper introduces a model for nonperturbative nonlinear optics involving continuum states. The model suggests ways of optimizing and controlling the high-order nonlinear susceptibility. In addition, it clarifies the connection between above-threshold ionization and harmonic generation. For example, the model shows that there is not a one-to-one correspondence between above-threshold-ionization peaks and harmonic emission. It also shows why the maximum energy of the harmonic emission is very different from the maximum above-threshold-ionization energy. However, the strength of the harmonic emission increases approximately linearly with the ionization rate.

The paper applies concepts long familiar to plasma physicists to strong-field atomic physics. Since the products of atomic ionization are the basic constituents of plasmas, we should not be surprised if plasma methods are applicable. High-field atomic physics and plasma physics are becoming increasingly entwined [1].

The essential point in the paper is that an atom that undergoes multiphoton ionization does not immediately become a well-separated electron and ion. Rather, there is a significant probability of finding the electron in the vicinity of the ion for one or more laser periods. This paper extends the quasistatic model of multiphoton ionization [2,3] to include the electron interaction with the ion. By doing so, the model is able to quantitatively predict double ionization [4], hot above-threshold ionization [5], and, most important, high-harmonic generation [6,7]. The paper presents a unified approach to all three phenomena. This is done using only one free parameter that is severely constrained. Furthermore, the parameter is subject to independent experimental and theoretical study.

The quasistatic model, as it has been applied, consists of a dual procedure which will now be outlined. First, one determines the probability of ionization as a function of the laser electric field using tunnel ionization models. For all calculations in this paper, the ionization rate is given by [8]

$$W_{dc}=\omega_s|C_{n^*l^*}|^2G_{lm}(4\omega_s/\omega_t)^{2n^*-m-1}\exp(-4\omega_s/3\omega_t)\,, \tag{1}$$

where $\omega_s=E_s^0/\hbar$, $\omega_t=e\mathcal{E}(2m_eE_s^0)^{-1/2}$, $n^*=(E_s^h/E_s^0)^{1/2}$, $G_{lm}=(2l+1)(l+|m|)!(2^{-|m|})/|m|!(l-|m|)!$, and $|C_{n^*l^*}|^2=2^{2n^*}[n^*\Gamma(n^*+l^*+1)\Gamma(n^*-l^*)]^{-1}$. In Eq. (1), E_s^0 is the ionization potential of the atom of interest, E_s^h is the ionization potential of hydrogen, l and m are the azimuthal and magnetic quantum numbers, and $\mathcal{E}$ is the electric field amplitude. The effective quantum number l^* is given by $l^*=0$ for $l\ll n$ or $l^*=n^*-1$ otherwise. The probability of ionization, $P(t)$, during the time interval dt is $P(t)=W_{dc}(\mathcal{E}(t))dt$, where $\mathcal{E}(t)$ is the magnitude of the electric field $\mathcal{E}(t)=\mathcal{E}_0\cos(\omega t)\mathbf{e}_x+\alpha\mathcal{E}_0\times\sin(\omega t)\mathbf{e}_y$. The tunneling model describes the formation of a sequence of wave packets, one near each peak of the laser electric field.

The second part of the quasistatic procedure uses classical mechanics to describe the evolution of an electron wave packet. For simplicity, we shall consider only the electric field of the laser. Both the magnetic field of the laser and the electric field of the ion, for example, are ignored. The initial conditions of velocity and position equal 0 (the position of the ion) at the time of ionization have been justified previously in the long wavelength limit [2] by the comparisons with above-threshold-ionization experiments. After tunneling, the electron motion in the field is given by

$$\begin{aligned}x&=x_0[-\cos(\omega t)]+v_{0x}t+x_{0x}\,,\\ y&=\alpha x_0[-\sin(\omega t)]+\alpha v_{0y}t+y_{0y}\,,\end{aligned} \tag{2}$$

$$v_x=v_0\sin(\omega t)+v_{0x},\quad v_y=-\alpha v_0\cos(\omega t)+v_{0y}\,, \tag{3}$$

where $\alpha=0$ for linearly polarized light and $\alpha=\pm1$ for circular polarization; $v_0=q\mathcal{E}_0/m_e\omega$, $x_0=q\mathcal{E}_0/m_e\omega^2$, and v_{0x}, v_{0y}, x_{0x}, and y_{0y} can be evaluated from the initial conditions (position and velocity equal to 0 at the time of tunneling). The energy associated with the velocities v_{0x} and v_{0y} constitute the above-threshold-ionization energy in ultrashort pulse experiments [2]. For circularly polarized light, Eq. (3) indicates that the electron trajectory never returns to the vicinity of the ion. Consequently, electron-ion interactions will not be important. This gives an opportunity to test this part of the model before proceeding.

0031-9007/93/71(13)/1994(4)$06.00

Recent experiment [9] and analysis [10] indicate that the quasistatic predictions are at least approximately valid for intensities as low as those having a ponderomotive energy equal to the ionization potential. Since the ultrashort pulse above-threshold-ionization spectrum for circularly polarized light is completely determined by Eqs. (1) and (3), precise verification of the quasistatic approach is possible. Because of space limitations, we can only summarize these findings here. There is excellent agreement between the quasistatic predictions and experimental [5] results published for above-threshold ionization of helium using 0.8 μm circularly polarized light. It is clear that Eq. (1) must accurately predict the sequential ionization rate. Such accurate predictions are essential for what follows, especially for calculations of the correlated two-electron multiphoton ionization rates. Having established the accuracy of Eqs. (1) and (3), we now discuss the implications for linearly polarized light.

Equations (1) and (2) show that half of the electrons that are field ionized by linearly polarized light pass the position of the ion ($x=0$) once during the first laser period following ionization. The other electrons will never pass the position of the ion. Equations (1)-(3) determine the probability, $P(E)$, per unit energy per laser period of finding an electron passing the ion with energy E. Figure 1 shows $P(E)$ obtained assuming uniform illumination, 5×10^{14} W/cm^2, 800 nm light interacting with helium. The most likely and the maximum velocity of an electron passing the nucleus corresponds to an instantaneous kinetic energy of 3.17 times the ponderomotive potential ($3.17U_p$). (As we shall see below, this is the physical origin of the $3.2U_p+E_s^0$ law for the high-harmonic radiation cutoff [6].) An electron ionized by tunneling at $\omega t\approx17°$, 197°, etc., will arrive at the ion with this velocity. Clearly it is inappropriate to ignore the interaction between the ion and this returning electron. We now discuss three aspects of this interaction.

One consequence of the electron-ion interaction can be immediately understood. If the energy of the electron as it passes the ion exceeds the e-$2e$ scattering energy, the *ion* can be collisionally ionized by the electron that has left the atom only a fraction of a period earlier. In other words, correlated two-electron ejection should be observed. Figure 2 shows the calculated ion yields obtained as a function of the laser intensity for 0.6 μm light interaction with helium. The agreement with published [4] experimental results is extremely good. To obtain this curve, the known collision cross section of He^+ was used [11]. The only free parameter in the model was the transverse spread of the electron wave function, or, equivalently, the range of possible impact parameters. For the data shown in Fig. 2 the wave function was assumed to have a Gaussian probability distribution for the impact parameter with a half intensity radius of 1.5 Å. Because of the presence of the strong laser field, inelastic scattering leading to excited states should also contribute to the experimental results since an atom in an excited state should immediately ionize. If inelastic scattering is included, the agreement is also good, provided that the radius is increased to $\sim$2 Å. Even at 2 Å, the transverse spread of the wave function is less than estimated previously [2] by comparing the long wavelength limit of Reiss' ionization model [12] with the quasistatic predictions. The origin of this discrepancy is unclear. It may be the result of neglecting spin correlation effects [13].

The electron can also scatter elastically. Any electron that scatters is dephased from its harmonic motion and therefore absorbs energy from the field. Following the same approach used to study inverse bremsstrahlung in plasma physics [14], we assume that $\tan(\chi/2)=P/P_c$, where χ is the angle of deviation of the electron, P is the

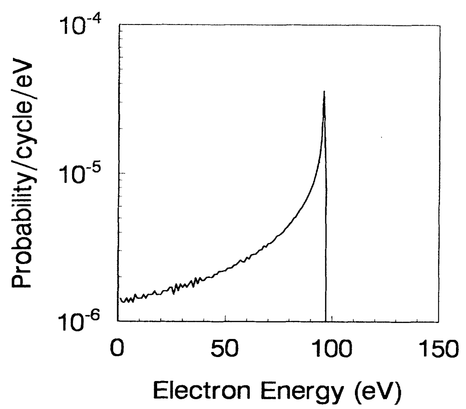

FIG. 1. Velocity distribution for electrons at the time of their first encounter with the ion. The parameters used for this calculation were those of helium with light intensity of 5×10^{14} W/cm^2 and wavelength 0.8 μm. The sharp cutoff in the electron energy occurs at $3.17U_p$.

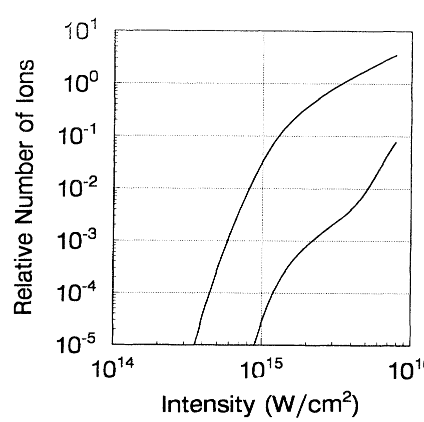

FIG. 2. Ion yield of singly (left curve) and doubly (right curve) charged ions plotted as a function of the peak laser intensity. The parameters were chosen to match those in Ref. [4], that is, ionization of helium with a $\sim$100 fs pulse of linearly polarized 0.6 μm light and a Gaussian spatial and temporal profile.

impact parameter, and P_c is the critical impact parameter given by $P_c = q^2/4\pi\varepsilon_0 m_e v^2$, with v the electron velocity as it passes the ion. This equation, which describes field-free scattering, should be a good approximation for large electron velocities and large impact parameters. Figure 3 was obtained by assuming that both the elastic and inelastic scattering angle could be approximated by the elastic scattering angle. For each moment of ionization t', the time t, velocity v, and probability of the electron passing the ion were determined using Eqs. (1)-(3). In the case of inelastic scattering, the scattered electron was assumed to lose sufficient energy to account for the ionization potential of He^+. The other electron was assumed to be produced with zero kinetic energy. The electron velocity after scattering was used as the initial condition in Newton's equation to determine the final above-threshold-ionization spectrum. The parameters used in Fig. 3 were those reported for published [5] above-threshold-ionization spectra obtained for helium using 0.8 μm light. Both the experiment and the model show that electrons with energy much greater than the ponderomotive energy (~ 100 eV) at the saturation intensity for helium are produced. Thus, there is qualitative, although not quantitative, agreement between calculation and experiment. With the use of differential scattering cross sections for helium, the model results can be improved. Indeed they should also allow predictions of the energy and angular dependence of correlated electron production.

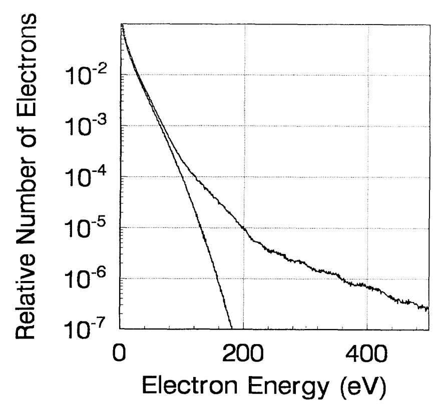

FIG. 3. Above-threshold-ionization electron energy spectrum. The relative number of electrons are plotted as a function of their energy. The calculations used parameters to match those in the experiment reported in Ref. [5], that is, ionization of helium with 0.8 μm linearly polarized light with a peak intensity of 4×10^{15} W/cm^2. A Gaussian spatial and temporal profile was assumed with a full-width-at-half-maximum pulse duration of ~ 100 fs. For reference, the spectrum with the electron scattering cross section of 0 is shown (left curve).

Another consequence of the electron-ion interaction is the emission of light. If the ground state is negligibly depleted, the wave packet will pass the ion in the same way during each laser cycle. Thus, any light that is emitted will be at a harmonic of the laser frequency.

The emission can be calculated from the expectation value of the dipole operator $\langle\psi|er|\psi\rangle$. If we assume that $\psi = \psi_g + \psi_c$, where ψ_g is the ground state wave function and ψ_c is the continuum wave function, then the dipole moment can be rewritten as $\langle\psi|er|\psi\rangle = \langle\psi_g|er|\psi_c\rangle + \langle\psi_c|er|\psi_c\rangle + \text{c.c.}$ To evaluate this integral, the following simplifications were made: (1) The ground state was negligibly depleted and was approximated by the ground state wave function of hydrogen. With this assumption, $\langle\psi_g|er|\psi_c\rangle + \text{c.c.}$ are the dominant terms and account for the high-harmonic radiation. (2) The continuum wave function was constructed using the correspondence principle. Since harmonic radiation of a given harmonic frequency $(E_h/\hbar)$ must come from electrons in an energy range $E_h - \hbar\omega < E < E_h + \hbar\omega$, it is convenient to write the wave function as it passes near the origin as

$$\psi_c(x \approx 0,t) = \sum_h A_p(x \approx 0,t)\exp[ip_h(x \approx 0,t)x/\hbar]\exp[-i\{p_h(x \approx 0,t)^2/(2m_e + E_s^0)t/\hbar\}] ,$$

where the index of the sum labels the harmonic and $p_h(x \approx 0,t)$ is the electron momentum that will lead to a given harmonic (A_p is defined below). (3) An electron born in the phase interval $\omega t < 17°$ can have the same energy passing the ion as one born in the interval $\omega t > 17°$. These contributions to the harmonic emission were added incoherently. (4) To obtain the normalization parameter A_p, the transverse spread r of the electron wave function was assumed to be linear in time with a magnitude of ~ 1.5 Å/fs. This spread is consistent with the two-electron ejection calculations (Fig. 2). The wave function spread in the direction of propagation was taken as the electron velocity $[p(x \approx 0)/m_e]$ multiplied by the time difference δt between the times when electrons of energy $E_h - \hbar\omega$ and $E_h + \hbar\omega$ pass the nucleus. The normalization condition was

$$\int A_p^2 d^3x = \left[\int_{E_h - \hbar\omega}^{E_h + \hbar\omega} P(E)dE\right] \Big/ V ,$$

where $V = \pi r^2 p \delta t/m_e$.

Figure 4 shows the calculated harmonic spectrum of the absolute value of the dipole moment squared, averaged over one period and measured in atomic units. The calculation was performed for 1 μm light interacting with helium. The parameters were chosen to be the same as those used in a recent Schrödinger equation simulation of high-harmonic generation [6]. Figure 4 bears a remarkable similarity to the results of the simulation. The plateau region has the same structure. They both begin at $\sim 10^{-6}$ atomic unit and decay in an extended plateau until a photon energy of ~ 225 eV, a value equal to 3.17 times the ponderomotive energy + the ionization poten-

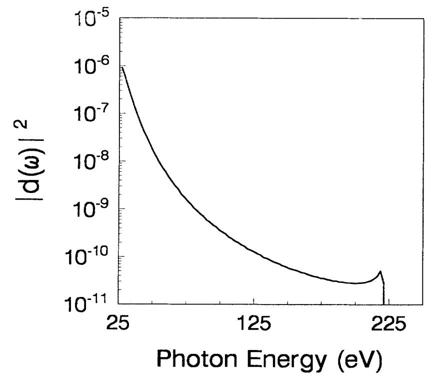

FIG. 4. Calculated value of the square of the dipole moment (measured in atomic units) plotted as a function of E_h of the harmonic. The calculation was performed for 1.06 μm fundamental radiation interacting with helium with an intensity of 6×10^{14} W/cm^2. The parameters were chosen to match those in Ref. [6].

tial. Even the magnitude of the high harmonics agrees within less than an order of magnitude. It is clear from this agreement that the quasistatic model catches the essence of high-harmonic generation.

Because of the simplicity of the quasistatic model, a number of issues are clarified. The high-frequency cutoff of the harmonic radiation depends on the ponderomotive energy because the maximum energy of the electrons responsible for harmonic emission is determined by the ponderomotive energy. Assuming that the ground state is not significantly depleted, the strength of the induced dipole moment at a given harmonic depends on the probability of an electron in the appropriate velocity range passing the ion. Consequently, it depends on the ionization rate. The dipole moment also depends on the transverse spread of the electron wave function. Assuming a constant rate of increase of the radial dimension of the electron wave function, the strength of the single atom response should vary quadratically with the inverse of the laser period. Clearly, harmonics will be generated most efficiently with the shortest pulses and the shortest wavelengths. The phase of the harmonic emission can be estimated within the quasistatic model by following the accumulated phase of the free electron over the classical path, $0.5\int(p/\hbar)dx$. Phase issues, however, will be discussed in another paper [15].

Finally, from a plasma perspective, the plasma collision frequency evolves transiently from a high value to the equilibrium plasma value. Thus, aspects of high density plasma physics will be found in low density ultrashort pulse laser produced plasma experiments. This extends the range of control of plasma parameters available using ultrashort pulse multiphoton ionization [1]. However, only a slight ellipticity of the laser polarization will ensure that the electron never returns to the environment of the ion—the conditions discussed previously [1] are recovered.

In conclusion, the transverse spread of the electron wave function is an important parameter which can be inferred from experiments using elliptically polarized light. Such experiments and their consequences will form an important new direction in strong-field atomic physics. Future experiments using linearly polarized light to study harmonic generation, double ionization, or above-threshold ionization will be of most value if the polarization of the laser pulse is known precisely.

This paper has benefited from invaluable discussions with many colleagues. These include M. Ivanov, N. H. Burnett, P. Dietrich, A. Zavriyev, A. Stolow, D. Villeneuve, M. Perry, K. Kulander, and L. DiMauro.

[1] P. B. Corkum, N. H. Burnett, and F. Brunel, in *Atoms in Intense Laser Fields,* edited by M. Gavrila (Academic, New York, 1992), p. 109.
[2] P. B. Corkum, N. H. Burnett, and F. Brunel, Phys. Rev. Lett. **62**, 1259 (1989).
[3] P. B. Corkum and P. Dietrich, Comments At. Mol. Phys. **28**, 357 (1993).
[4] D. N. Fittinghoff *et al.*, Phys. Rev. Lett. **69**, 2642 (1992).
[5] U. Mohideen *et al.*, Phys. Rev. Lett. **71**, 509 (1993).
[6] J. L. Krause, K. J. Schafer, and K. C. Kulander, Phys. Rev. Lett. **68**, 3535 (1992).
[7] J. J. Macklin, J. D. Kmetec, and C. L. Gordon III, Phys. Rev. Lett. **70**, 766 (1993).
[8] M. V. Ammosov, N. B. Delone, and V. P. Krainov, Zh. Eksp. Teor. Fiz. **91**, 2008 (1986) [Sov. Phys. JETP **64**, 1191 (1986)].
[9] S. Augst *et al.*, Phys. Rev. Lett. **63**, 2212 (1989).
[10] F. A. Ilkov, J. E. Decker, and S. L. Chin, J. Phys. B **25**, 4005 (1992).
[11] H. Tawara and T. Koto, At. Data Mol. Data Tables **36**, 167 (1987).
[12] H. R. Reiss, Phys. Rev. A **22**, 1786 (1980).
[13] I. E. McMarthy and E. Weigold, Adv. At. Mol. Phys. **27**, 201 (1991).
[14] E. H. Holt and R. E. Haskell, *The Foundations of Plasma Dynamics* (Macmillan, New York, 1965), p. 92.
[15] M. Lewenstein *et al.* (to be published).